diameters, it is expected that the activation energy necessary to dilate the indium lattice to allow the solute atoms to diffuse from one interstitial site to another will be the same for both atoms. However, in apparent contradiction of this simple picture, the experimental diffusion activation energies are 7 kcal/mole for gold and 12 kcal/mole for silver. One model which may explain this anomaly is that silver solute atoms are distributed between substutional and interstitial sites in indium whereas gold dissolves largely interstitially. Thus the additional 5 kcal/mole necessary for the silver diffusion would represent the energy that is required to activate silver from a substitutional to an interstitial site before silver interstitial diffusion could occur. In contrast, gold being dissolved entirely interstitially would need only 7 kcal/mole of activation energy for diffusion, the work required by both the equally sized gold and silver atoms to jump from one interstitial site in the indium lattice to another. Hence, on the basis of this tentative model, gold would dissolve and diffuse wholly interstitially while the diffusion of silver in indium would be best described by the dissociative mechanism proposed by Frank and Turnbull.[17]

As a final comment, it should be mentioned that theoretical considerations and diffusion results for other systems indicate that copper should also dissolve interstitially in indium and that it should diffuse faster than both gold and silver.

ACKNOWLEDGMENT

The authors are grateful to Dr. B. F. Dyson for helpful suggestions about the experimental work.

[17] F. C. Frank and D. Turnbull, Phys. Rev. **104**, 617 (1955).

PHYSICAL REVIEW VOLUME 151, NUMBER 2 11 NOVEMBER 1966

Theory of the Galvanomagnetic Properties of Magnesium and Zinc

L. M. FALICOV*
Cavendish Laboratory, University of Cambridge, Cambridge, England
and
Department of Physics and Institute for the Study of Metals, University of Chicago, Chicago, Illinois†
AND
A. B. PIPPARD
Cavendish Laboratory, University of Cambridge, Cambridge, England
AND
PAUL R. SIEVERT‡
Department of Physics and Institute for the Study of Metals, University of Chicago, Chicago, Illinois

(Received 16 May 1966)

A theory of the galvanomagnetic properties of magnesium and zinc is developed. It is restricted to magnetic fields parallel to the hexad axis and takes into account the effects of magnetic breakdown. The transverse magnetoresistance shows the expected transition from electron-hole compensation at low fields to a noncompensated state at high fields, i.e., a transition from quadratic behavior to saturation. The Hall resistance shows the corresponding behavior. In addition, all transverse components of both conductivity and resistivity tensors show strong oscillations of the de Haas–van Alphen type due to coherent effects in the tunneling probability through small pieces of the Fermi surface. Theoretical curves are shown for various components of the galvanomagnetic tensors and compared with experimental measurements. Most parameters involved in the comparison are provided, or at least checked, by other experiments; only the breakdown field strength H_0 is unknown. It is found that a single H_0 suffices for Zn, but that for Mg, H_0 varies along the hexad axis. With this limited degree of adjustability, good agreement may be obtained between theory and experiment, though minor discrepancies remain unexplained.

1. INTRODUCTION

THE hexagonal-close-packed (hcp) metals Zn,[1–3] Mg,[4–6] and Be[7] show remarkable galvanomagnetic properties which depart drastically from those usually found in metals. As is well known[8] the transverse magnetoresistance commonly exhibits, for single-

* Alfred P. Sloan Research Fellow.
† Work supported in part by the National Science Foundation and the U. S. Office of Naval Research.
‡ Advanced Research Projects Agency Research Assistant.
[1] R. W. Stark, Phys. Rev. Letters **9**, 482 (1962); Phys. Rev. **135**, A1698 (1964).
[2] N. E. Alekseevskii and Yu. P. Gaidukov, Zh. Eksperim. i Teor. Fiz. **43**, 2094 (1962) [English transl.: Soviet Phys.—JETP **16**, 1481 (1963)].
[3] W. A. Reed and G. F. Brennert, Phys. Rev. **130**, 565 (1963).
[4] R. W. Stark, T. G. Eck, and W. L. Gordon, Phys. Rev. **133**, A443 (1964).
[5] R. W. Stark, in *Proceedings of the IXth International Conference on Low Temperature Physics, Columbus, Ohio 1964* (Plenum Press, Inc., New York, 1965), p. 712.
[6] R. W. Stark (private communication).
[7] W. A. Reed, Bull. Am. Phys. Soc. **9**, 633 (1964), and private communication.
[8] For complete reviews of the general theory and experimental situation of the galvanomagnetic effects in metals see for instance R. G. Chambers, in *The Fermi Surface*, edited by W. A. Harrison and M. B. Webb (John Wiley & Sons, Inc., New York, 1962), p. 100; E. Fawcett, Advan. Phys. **13**, 139 (1964) and the many references quoted there.

crystal specimens and high magnetic fields, two types of functional dependence on the field strength: either a saturation at a constant value ($\rho_\perp \to$ constant) or a quadratic increase ($\rho_\perp \propto H^2$). These dependences of $\rho_\perp$ on H have been interpreted in terms of the topological properties of the energy surfaces[9]; the interpretation assumes a semiclassical approach, i.e. the electrons are considered as "classical" particles which obey a general dispersion law $\epsilon(k)$ and Fermi-Dirac statistics. In addition, the quantization of the magnetic orbits (Landau levels) is responsible for the appearance in some cases of rather weak oscillations (de Haas-Schubnikov effect), periodic in H^{-1}.

The divalent hexagonal metals, magnesium and zinc in particular, exhibit a very different behavior as can be seen from Figs. 1 and 2. The curves for the transverse magnetoresistance for fields parallel to the hexad axis show an initial quadratic increase up to a maximum value, reached at about 3–4 kG, and then a decrease in the resistivity by a factor of about 3 down to an apparent saturation at very high magnetic fields. Superimposed on this general behavior there are very strong oscillations, periodic in H^{-1}, with an amplitude and period much larger in Zn than in Mg.

Two features of these curves need explanation: (a) the transition from quadratic character to saturation, with the appearance of a maximum, and (b) the unusually large amplitude of the oscillations. Both effects can be explained in terms of magnetic breakdown,[10–16] i.e. in terms of a model that allows transitions

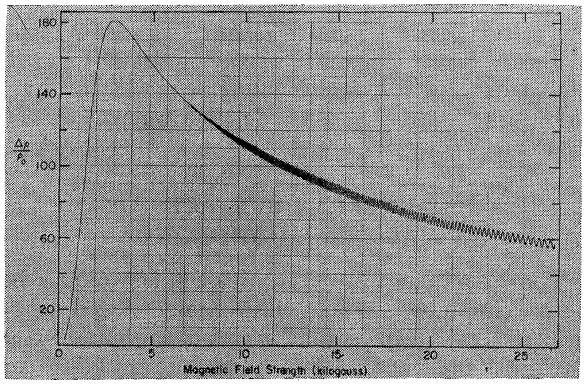

FIG. 1. A typical experimental curve for the transverse magnetoresistance in Mg for a magnetic field direction parallel to the hexad axis. The curve was taken by R. W. Stark (Refs. 5 and 6) in extremely high-purity Mg and does not include corrections for possible Hall effect contributions.

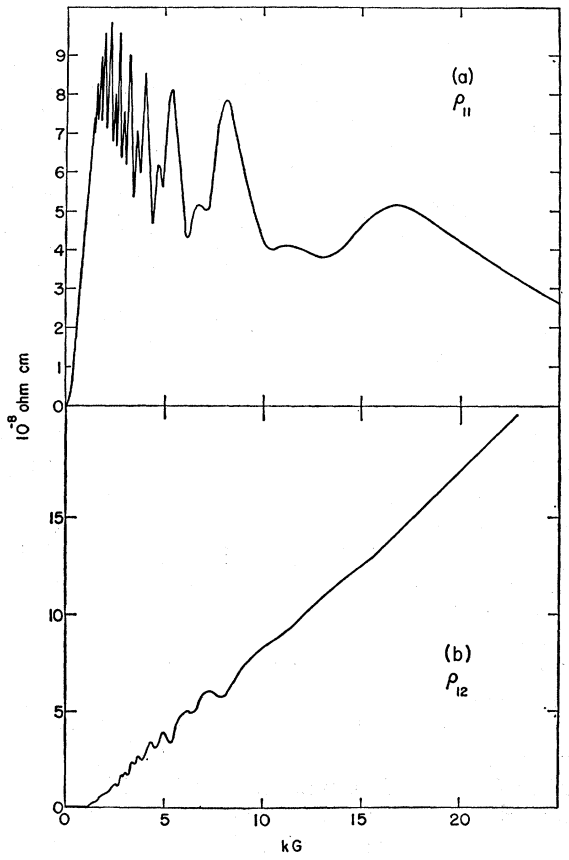

FIG. 2. Experimental curves for the transverse magnetoresistance and the Hall resistance in Zn for a magnetic-field direction parallel to the hexad axis. The curves were taken by R. W. Stark (Ref. 1) and correspond to $T=1.6$°K. (a) Transverse resistivity, (b) Hall resistivity.

between various pieces of the Fermi surface. The probability of transition is given by[10,11]

$$P=\exp[-H_0/H], \tag{1.1}$$

where

$$H_0=K\Delta^2 mc/\epsilon_F \hbar e; \tag{1.2}$$

ϵ_F is the Fermi energy, Δ is the energy gap separating the two energy bands from which the two sheets of Fermi surface originate, and K is a numerical factor of order 1. Discussing his zinc data, Stark[1] suggested that the probability of transition between a large portion of the Fermi surface and a second small portion might be modulated by the quantized Landau levels of the small piece. He also interpreted the complex structure of the oscillations in terms of the spin splitting of the Landau levels. He did not however attempt a quantitative development of his ideas.

[9] I. M. Lifshitz, M. Ya. Azbel, and M. I. Kaganov, Zh. Eksperim. i Teor. Fiz. **30**, 220 (1955); **31**, 63 (1956) [English transls.: Soviet Phys.—JETP; **3**, 143 (1956); 4, 41 (1957)] I. M. Lifshitz and V. G. Peschanskii, Zh. Eksperim. i Teor. Fiz. **35**, 1251 (1958); **38**, 188 (1960) [English transls.: Soviet Phys.—JETP **8**, 875 (1959); **11**, 137 (1960)].

[10] M. H. Cohen and L. M. Falicov, Phys. Rev. Letters **7**, 231 (1961).

[11] E. I. Blount, Phys. Rev. **126**, 1636 (1962).

[12] M. G. Priestley, L. M. Falicov, and G. Weisz, Phys. Rev. **131**, 617 (1963).

[13] A. B. Pippard, Proc. Roy. Soc. (London) **A270**, 1 (1962).

[14] A. B. Pippard, Phil. Trans. Roy. Soc. London **A256**, 317 (1964).

[15] A. B. Pippard, Proc. Roy. Soc. (London) **A287**, 165 (1965).

[16] L. M. Falicov and P. R. Sievert, Phys. Rev. Letters **12**, 550 (1964); Phys. Rev. **138**, A88 (1965).

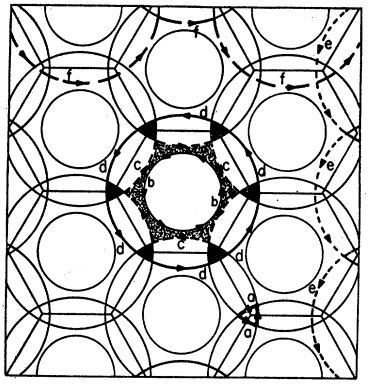

FIG. 3. Schematic cross section of the Fermi surface of the divalent hcp metals with a plane normal to the c axis. The full triangles correspond to the "needles" and the shaded hexagon to the "monster." Various possible orbits are indicated.

Two possible approaches to a more systematic study of the phenomenon can be taken. The first, which has been followed by one of the authors,[14,15] starts from a complete quantum-mechanical description of the system. This description results in a new magnetic level band structure,[14] from which new excitations or quasiparticles with definite quasimomentum and energy can be defined; they are responsible for all transport properties of the material at high magnetic fields. This extreme quantum approach presents two difficulties, one from the conceptual and computational points of view and a second of experimental nature. The first problem arises from the fact that the quasiparticles are only properly defined when the magnetic flux contained in a unit cell is a rational fraction of the flux quantum hc/e, and only susceptible of a not too cumbersome computational handling when it is an integral multiple of hc/e.[14] Recent work[17] on nonintegral multiples has shown clearly that the original estimate[14] of quasiparticle conductivity was greatly in excess of what may be expected as an average over even quite a narrow range of magnetic field strength. The second difficulty originates from the fact that a very low density of lattice imperfections, particularly dislocations, introduces phase incoherence, which results in a partial or total randomization of the network,[15] thus scattering the quasiparticles to such an extent that their very existence is threatened.

The second approach, followed by the other two authors,[16] starts from a completely semiclassical picture in which no phase coherence is taken into account; the electrons are pictured as Fermi-Dirac particles satisfying Boltzmann's equation in a random walk through a network. At each junction in the network the electrons continue in their free-electron (circular) path with probability P, given by Eq. (1.1) or are Bragg reflected to another free-electron orbit with probability

$$Q=1-P. \tag{1.3}$$

This approach, which is entirely semiclassical, can thus give no explanation for the oscillations; it is however, very successful in explaining the over-all behavior of the magnetoresistance and Hall resistance curves. It is worth pointing out that this picture is probably identical with the quantum-mechanical picture if complete randomization is included.[15]

The experiments reported on zinc and magnesium are evidently in an intermediate range, where randomization has taken place in the large orbits of the network but coherence effects remain for some very small orbits, those responsible for the observed oscillations. This intermediate case can be solved by dividing the network into two parts, a classical part where the Boltzmann equation is to be solved, and a small "quantum-mechanical" part responsible for the "switching" probabilities at the various junctions of the classical network. Within the small part all coherence effects are taken into account and consequently the probabilities of transition are modulated with the characteristic frequencies of the small orbits.

Before entering the detailed description of the theory, it is worth pointing out that the experimental data at very high magnetic fields show a rather weak dependence on either the temperature or the purity of the sample, indicating that the principal scattering mechanism for the electrons is provided by magnetic breakdown,[16] so that the mean free path of the quasiparticles is limited by effects other than temperature and purity. This fact also justifies our simplification of assuming that for those parts of the Fermi surface which break down at high magnetic field, the intrinsic relaxation time (or mean free path) can be considered infinite.

In the following section we review briefly those details of the Fermi surface which are of relevance for our calculation. Section 3 is devoted to a brief review of theory of the transverse magnetoresistance and the Hall effect for the hexagonal network in the intermediate regime. In Sec. 4 a detailed comparison with experiment is carried out.

2. THE FERMI SURFACES OF MAGNESIUM AND ZINC

The Fermi surface of the divalent hcp metals has been well established both theoretically[18,19] and experimentally.[20–22] Of the several sheets of the surface, only two are of interest for our purposes: (i) A multiply connected region in the second band which contains holes and has been referred to in the literature as the "monster"; (ii) two singly connected electron surfaces in the third zone of elongated shape (longest dimension parallel to the c axis) and referred to as the "needles" (Zn) or the "cigars" (Mg).

A schematic cross section of these two pieces with a plane normal to the c axis and passing through the

[17] W. G. Chambers, Phys. Rev. **140**, A135 (1965).

[18] L. M. Falicov, Phil. Trans. Roy. Soc. (London) **A255**, 55 (1962).
[19] W. A. Harrison, Phys. Rev. **126**, 497 (1962).
[20] M. G. Priestley, Proc. Roy. Soc. (London) **A276**, 258 (1963).
[21] A. S. Joseph and W. L. Gordon, Phys. Rev. **126**, 489 (1962).
[22] D. F. Gibbons and L. M. Falicov, Phil. Mag. **8**, 177 (1963).

TABLE I. Parameters of the Fermi surface of magnesium and zinc.[a]

	Mg	Zn
Fermi momentum	0.727[b]	0.841[c]
Cross-sectional area of the Brillouin zone	1.255[b]	1.815[c]
Cross-sectional area of the free-electron sphere A_0	1.66[b]	2.22[c]
Cross-sectional area of the "needles" A_{T0}	6.49×10^{-3} [d]	4.24×10^{-5} [e]
Height of the "needles"	$\sim5.5\times10^{-1}$ [b]	$\sim1.2\times10^{-1}$ [f]
Cross-sectional area of horizontal arms of "monster"	7.32×10^{-3} [d]	1.2×10^{-3} [e]
Approximate height of "monster waist" $2k_{zm}$	$\sim1\times10^{-1}$ [g]	$\sim4\times10^{-2}$ [g]
$\gamma=\partial A_T/\partial(k_z^2)$	-2.76×10^{-1} [h]	-1.13×10^{-2} [f] -1.77×10^{-2} [h]

[a] All parameters in atomic units.
[b] Reference 18.
[c] Reference 19.
[d] Reference 20.
[e] Reference 21.
[f] Assuming the needles to be ellipsoidal.
[g] Assuming a circular cross section.
[h] Assuming the needles to be the intersection of three spheres.

center Γ of the Brillouin zone is given in Fig. 3. It is seen that if the inner boundary (orbit b) of the monster is neglected, all the other boundaries can be approximated by a network formed by circles centered at all the Γ points and with radii equal to the free-electron Fermi momentum. More details of the parameters of the Fermi surfaces of Mg and Zn are given in Table I.

The points in k space where magnetic breakdown occurs are those where the corners of the triangular section of the needles meet the corners of the hexagonal section of the monster. If no breakdown occurs, i.e. $P=0$, only the orbits indicated in Fig. 3 by a and c (in addition to the orbit b of the inner part of the monster) exist. In the other limit, i.e. for complete breakdown $P=1$, only the free electron circle d is present. As is easily seen, an electron a orbit and a hole c orbit change as H increases into one larger electron d orbit, thus destroying the compensation of electrons and holes which exists when $P=0$. It is the failure of compensation which provides the mechanism for the unusual magnetoresistive properties.

If successive parallel cross sections are taken at different heights k_z from Γ, similar networks are found only up to a very small value k_{zm}; there the orbit c meets the orbit b at their points of closest proximity. For $k_z>k_{zm}$ the "waist" (horizontal arms) of the monster has disappeared, giving rise to six oblique disconnected arms, and although magnetic breakdown between the needles and the oblique arms still may occur, the character of the orbits is no longer changed, i.e. sections with $k_z>k_{zm}$ do not contribute to variations in the numbers of electrons and holes. It can be seen from Table I that the total height of the monster waist is considerably smaller than the total height of the needles in both Mg and Zn, so that only a small central section of the needles has to be taken into account in analyzing the consequences of magnetic breakdown.

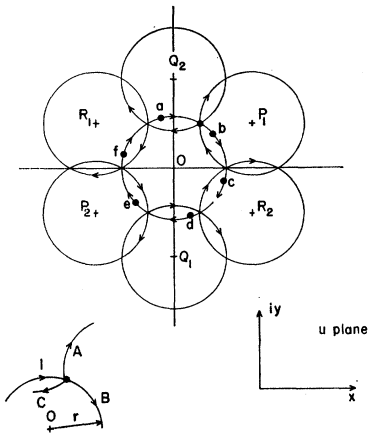

FIG. 4. A schematic representation of the hexagonal network in which the triangular orbits have been reduced to a three-way switching junction.

The orbits indicated a in Fig. 3 are the only ones which seem in practice to be small enough to retain phase coherence. The cross-sectional areas of these triangular orbits A_T are orders of magnitude smaller than any of the other areas involved in the problem, namely the circular or hexagonal orbits (see Table I). Consequently only the triangular orbits of the needles are considered in the small or quantum-mechanical part of the network, and along them phase coherence will be fully taken into account. The rest of the network, with the needle orbits shrunk to a point, is the large, semiclassical network used to solve Boltzmann's equation. A schematic representation of the semiclassical network is shown in Fig. 4. Each junction is now a three-way switch and one electron arriving at the junction with a total probability 1, may leave the junction through three different paths with probabilities A, B and C (Fig. 4). It has been proved[15] that the addition of amplitudes and phases[14] in the triangular "leaky" orbits yields for the probabilities

$$\begin{aligned} A&=1-B-C,\\ B&=P^2[1+Q^3-2Q^{3/2}\cos\phi]^{-1},\\ C&=BQ, \end{aligned} \tag{2.1}$$

where P and Q are given by (1.1), (1.2) and (1.3), and ϕ is, except for a constant, the phase change of electrons when traveling around the needle orbit once, i.e.

$$\phi(k_z)=\hbar cA_T/eH-\phi_0. \tag{2.2}$$

Here $A_T(k_z)$ is the area of the orbit in k space and ϕ_0 is a constant phase. Values of A_{T0}, i.e. A_T for $k_z=0$ are given in Table I.

At this point it is worth noticing that randomization of the phases in this orbit is equivalent to averaging A, B and C over all values of ϕ. This averaging yields

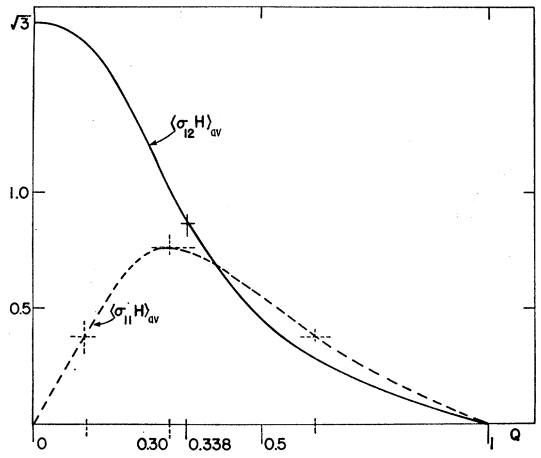

FIG. 5. The average value of the conductivity $\langle\sigma H\rangle_{av}$ in units of β as a function of Q.

immediately

$$A_c=1-B_c-C_c,$$
$$B_c=P^2[1-Q^3]^{-1}, \tag{2.3}$$
$$C_c=QB_c,$$

which are identical to the semiclassical formulas (3.4) of Ref. 16.

We can now define clearly the model that we take to compute the galvanomagnetic effects in Mg and Zn. We separate the free-electron sphere into a central section of thickness $2k_{zm}$ and the rest; the central section is now replaced by a system of semiclassical networks, as in Fig. 4, while the rest is treated in the normal way as if breakdown did not occur. The probabilities at the junctions, A, B and C, are given by (2.1), (1.1) and (1.3). It is found to be adequate to assume that H_0 is constant in zinc throughout the slab, but not in magnesium. In (2.2), however, the area A_T varies with height k_z, satisfying a relationship of the form

$$A_T(k_z)=A_{T0}+\frac{\partial A_T}{\partial(k_z^2)}k_z^2 \tag{2.4}$$

for $k_z<k_{zm}$. Values of the quadratic coefficients are given in Table I. It should be emphasized that the central section constitutes a very small portion of the Fermi surface (6% in Mg, 3% in Zn) whose contribution to the conductivity at low magnetic fields is correspondingly small. At high magnetic fields, however, the central section dominates the conductivity, especially for the very pure samples of Stark's experiments.[1,5,6] The reason for this is that at high fields the conductivity σ_{11} of electrons executing closed orbits is inversely proportional to their relaxation time. The electrons on the network have a very short effective relaxation time owing to the choice of paths at each junction, and consequently retain a high conductivity while that of the other electrons falls to a low value. It is this that permits us to concentrate attention on the network, and as a first approximation express the high-field conductivity of the rest of the electrons by a single empirically determined term α/H^2.

In Sec. 4, when comparing our theory with experiment, we have only made use of the data obtained by Stark,[1,5,6] which constitute in our opinion the most reliable and detailed set of experimental curves, and the only ones taken with the necessary sensitivity.

Before leaving this section it should be mentioned that those electronic states in the Zn structure responsible for the third-band needles have a very strong spin-orbit interaction. This results in an anomalously large g factor[23] which, as we shall see, leads to the double-peaked line shape of the oscillations in the magnetoresistance at large values of the magnetic field.

3. CALCULATION OF THE GALVANOMAGNETIC TENSORS

The calculation of the conductivity tensor in a semiclassical network (or in other words the solution of Boltzmann's equation for a system with magnetic breakdown) can be performed by two different methods which yield identical results:

(a) A matrix modification of Chambers' path integral method.[16]

(b) The effective-path method, proposed by one of the authors[24] in another connection and already developed for the hexagonal network with infinite relaxation time.[15]

In this paper we use mostly the effective path method and in particular the results quoted in Ref. 15.

The results of Ref. 15 can be summarized as follows. If we (1) use a complex system of co-ordinates in two dimensions (see Fig. 4)

$$u=x+iy, \tag{3.1}$$

(2) assume that the magnetic field is in the z direction, perpendicular to the u plane and the electric field in the x direction, i.e.

$$E=\mathrm{Re}E, \tag{3.2}$$

and (3) define for that case a complex conductivity σ

$$\sigma=\sigma_{xx}-i\sigma_{yx}=\sigma_{11}-i\sigma_{21}, \tag{3.3}$$

then the contribution of each infinitesimal section dk_z to the conductivity is

$$d\sigma=\frac{nec}{H}\left\{\frac{3}{\pi}\left[\eta^2+\frac{\eta}{1-\sqrt{3}iB(\eta+Q)}\right]+i\right\}dk_z, \tag{3.4}$$

where

$$\eta=\exp(-i\pi/3)=\tfrac{1}{2}-i\sqrt{3}/2, \tag{3.5}$$

[23] A. J. Bennett and L. M. Falicov, Phys. Rev. **136**, A998 (1964).
[24] A. B. Pippard, Proc. Roy. Soc. (London) **A282**, 464 (1964).

and ndk_z is the number of electrons per unit volume in the section.[25] The rest of the Fermi surface, i.e. that part not involved in magnetic breakdown, contributes to the conductivity in two ways:

(1) By adding to σ_{11} a term which arises from all closed orbits with finite relaxation time. For magnetic fields such that $\omega_c\tau \gg 2\pi$ this contribution is of the form[26] α/H^2.

(2) By adding to σ_{21} a term which ensures, for $Q \to 1$, complete compensation of electrons and holes, i.e., $\sigma_{21} \to 0$. This compensation is achieved in (3.4) by replacing the term i within the brackets by $i3\sqrt{3}/\pi$.

Finally the total conductivity of the metal is given by

$$\sigma=\frac{1}{H}\int_0^{k_{zm}}\frac{6nec}{\pi}\left\{\eta^2+\frac{\eta}{1-\sqrt{3}iB(\eta+Q)}+i\sqrt{3}\right\}dk_z+\alpha/H^2. \tag{3.6}$$

The only important dependence of the integrand on k_z is through B, which depends on ϕ and thus on $A_T(k_z)$.[27] Both B and Q may vary slowly with k_z if H_0 depends on k_z.

Two further points are of interest. The first is the determination of $\bar{\sigma}$, the conductivity averaged over the phases. A straightforward but tedious integration yields

$$\langle\sigma H\rangle_{\rm av}=-\beta M\eta[(M+N)^2-1]^{-\frac{1}{2}}+\frac{\alpha}{H}, \tag{3.7}$$

where

$$\beta=\int_0^{k_{zm}}\frac{6nec}{\pi}dk_z \tag{3.8}$$

$$M=(\sqrt{3}/2)i(\eta+Q)P^2Q^{-3/2} \tag{3.9}$$

and

$$N=-\tfrac{1}{2}(1+Q^3)Q^{-3/2}. \tag{3.10}$$

A plot of the first term in (3.7) as a function of Q is given in Fig. 5. It is seen that the real part, $\langle\sigma_{11}H\rangle_{\rm av}$, takes the value zero at $Q=0$ and $Q=1$ and reaches a maximum at $Q_M\approx 0.30$ which corresponds to $H_M \doteqdot 2.82H_0$. The imaginary part $\langle\sigma_{21}H\rangle_{\rm av}$ on the other hand starts from a maximum value $\sqrt{3}\beta$ at $Q=0$ and falls off to zero at $Q=1$, reaching half its initial value at $Q_h \doteqdot 0.338$, $H_h \doteqdot 2.44H_0$. These curves are used in the next section to determine the parameters H_0, α and β in the actual cases.

The second point of interest is a convenient approximate way of evaluating the integral over k_z for the case when $H \ll \hbar cA_T/2\pi e$, so that ϕ is many times greater than 2π, a condition which, as we shall see in the next section, applies to the experimental situation in Mg but not in Zn. In the latter case (3.6) must be integrated numerically, but in the former the integration can be done by means of vector addition in the amplitude-phase diagram (Cornu spiral).[26] If the area $A_T(k_z)$ satisfies a quadratic relationship of the form (2.4), and if the oscillatory contribution to the conductivity of any section is a simple sinusoidal function of A_T, the total oscillatory conductivity is the same as if only a central portion were engaged, and all with the same phase $\phi(0)-\frac{1}{4}\pi$. The width W of the central portion is such that ϕ ranges from $\phi(0)$ at the center to $\phi(0)-\frac{1}{4}\pi$ at the extremes. From (2.2) and (2.4)

$$W=(\pi eH/\hbar c\gamma)^{1/2} \tag{3.11}$$

in which

$$\gamma=\partial A_T/\partial(k_z^2).$$

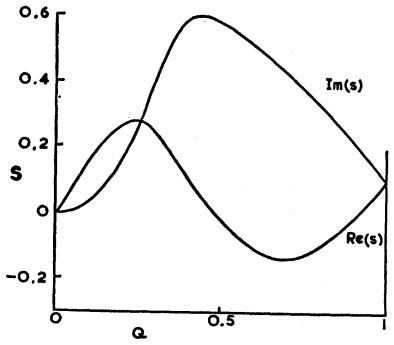

FIG. 6. Fundamental amplitude $s(Q)$ of the oscillatory part of the conductivity.

Now in fact the oscillatory term in (3.4) is not sinusoidal, and each harmonic should be evaluated separately. But because of the rather high frequency of the oscillations in Mg, and the temperature damping of the higher harmonics, what is observed is so closely sinusoidal that there is no need to consider more than the fundamental oscillation, $\Delta\sigma$, and superpose this on the average conductivity $\bar{\sigma}$. Hence the bracketed function (3.4) has been Fourier-analyzed for different values of Q and its fundamental amplitude s, determined, as shown in Fig. 6. Substituting W for dk_z in (3.4) we have

$$H\Delta\sigma=necWs\cos[\phi(0)-\tfrac{1}{4}\pi]. \tag{3.12}$$

This expression has been derived without paying attention to temperature-damping which, just as in the de Haas–van Alphen effect, is caused by the Fermi tail extending over more than one quantized level. The factor ζ by which the oscillatory amplitude $\Delta\sigma$ is to be multiplied is the same as in the de Haas–van Alphen effect,

$$\zeta=X/\sinh X, \tag{3.13}$$

where

$$X=2\pi^2m^*ckT/(\hbar eH),$$

and m^* is the cyclotron mass of the orbit responsible for the oscillations (cigar or needle).

[25] In (3.4), as elsewhere, e and H are to be taken as positive. The sign convention adopted in (3.3) does not agree with that of Ref. 15, but is chosen so that a preponderance of electrons, which is what we have in Zn and Mg, leads to a positive value of σ_{21}.

[26] See for instance, A. B. Pippard, Rept. Progr. Phys. 23, 176 (1960).

[27] In actual fact n and H_0 are also functions of k_z. The dependence of n on k_z is very weak and can be neglected. The assumption of an H_0 independent of k_z is only a good first approximation which greatly simplifies the calculations; its validity is discussed in Sec. 4.

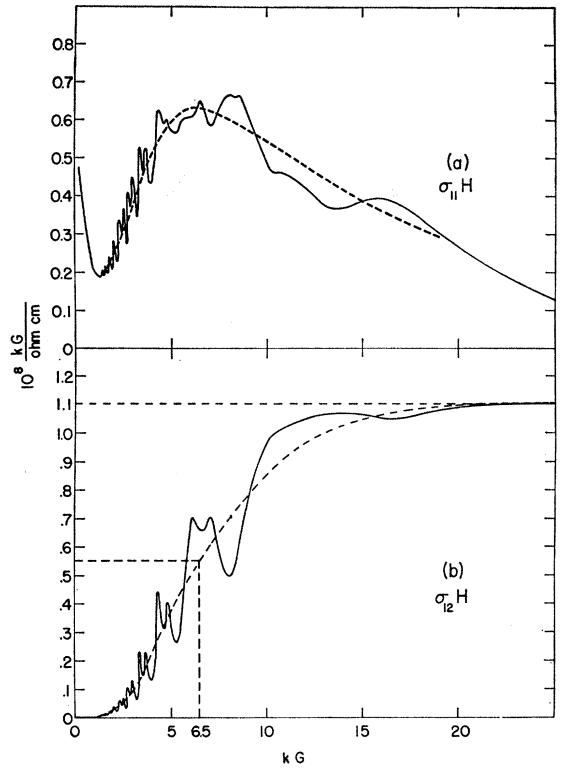

FIG. 7. The components of the product of conductivity tensor and the magnetic field strength for Zn. The curves were obtained by direct inversion of the experimental results of Fig. 2. (a) The diagonal components $\langle\sigma_{11}H\rangle_{av}=\langle\sigma_{22}H\rangle_{av}$. (b) The off-diagonal components $\langle\sigma_{12}H\rangle_{av}=\langle-\sigma_{21}H\rangle_{av}$. The dashed lines indicate the average values $\langle\sigma_{11}H\rangle_{av}$ and $\langle\sigma_{12}H\rangle_{av}$, the saturation value $(\langle\sigma_{12}H\rangle_{av})_S$ and the midpoint $\frac{1}{2}(\langle\sigma_{12}H\rangle_{av})_S$.

4. COMPARISON WITH EXPERIMENT

A. Zinc

In Fig. 2 we have shown the transverse magnetoresistivity ρ_{11} and the Hall resistivity ρ_{12} in a Zn sample as determined by Stark.[1] Since the calculations are performed in terms of the conductivities rather than the resistivities, we show in Fig. 7 the σH tensor obtained by inverting Fig. 2. The detailed comparison of these curves with the theoretical estimates is done in two steps; by averaging over the oscillations first and determining the parameters H_0, α and β, and then including the oscillations in the second step.

(i) *Nonoscillatory Behavior and Determination of the Parameters*

In Fig. 7(b) we have plotted, superimposed on $\sigma_{21}H$, the average value $\langle\sigma_{21}H\rangle_{av}$ obtained numerically from the experimental data. The curve tends to a saturation value of 1.10×10^8 $(\Omega\ \text{cm})^{-1}$. It reaches its half value at a value of $H_h=6.5$ kG. Comparison with the theoretical curve (Fig. 5) yields a value

$$H_0=2.7\ \text{kG} \tag{4.1}$$

for the breakdown-field parameter which enters Eq. (1.1). A check on this parameter is provided by the position of the maximum of $\langle\sigma_{11}H\rangle_{av}$. Since this is rather broad [Fig. 7(a)] and is not clearly defined because of the oscillations, the accuracy of this determination is not as reliable as what is obtained from $\langle\sigma_{21}H\rangle_{av}$. A value of $H_0=2.7$ kG gives, according to Fig. 5 and the discussion of Sec. 3, a value $H_M=7.6$ kG for the position of the maximum, which is in very good agreement with Fig. 7(a). The other parameters needed are

$$\alpha=0.17\times10^8(\text{kG})^2/\Omega\ \text{cm},$$
$$\beta=0.67\times10^8\ \text{kG}/\Omega\ \text{cm}, \tag{4.2}$$

which were also determined by comparison with experiment. If (4.1) and (4.2) are inserted in (1.1), (1.3) and (3.7)–(3.10), the resulting curves for $\langle\sigma H\rangle_{av}$ are those shown in Fig. 8. The agreement is not perfect, but in view of the simplifications used in the theory it may be regarded as rather satisfactory.

The magnitudes of the parameters deserve comment. First we note that at fields less than 1 kG, where breakdown effects are very small, zinc should behave as a compensated metal with zero Hall angle (as observed) and $\rho_{11}=1/\sigma_{11}=H^2/\alpha$, provided $\omega_c\tau\gg1$. Thus we expect the resistivity in the low-field quadratic region to be

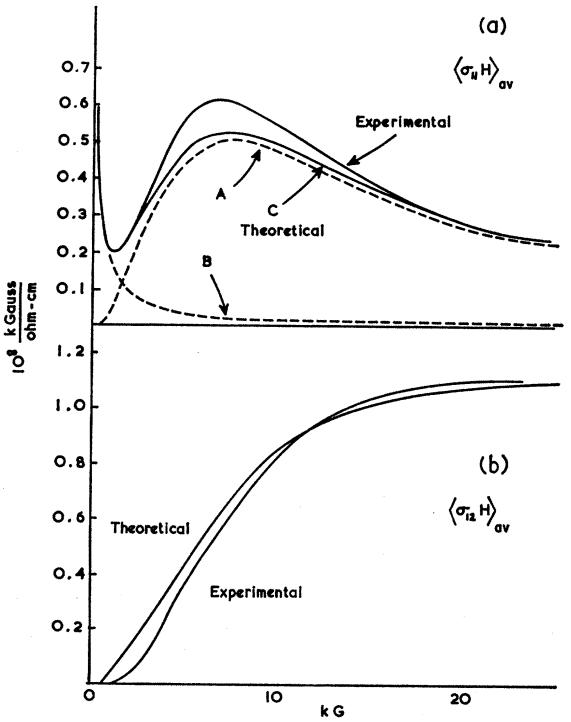

FIG. 8. The theoretical estimates for the average $\langle\sigma H\rangle_{av}$ for Zn. (a) The diagonal components $\langle\sigma_{11}H\rangle_{av}=\langle\sigma_{22}H\rangle_{av}$. A represents the contribution of the cylindrical slab which undergoes magnetic breakdown, B is the contribution of the rest of the Fermi surface and C is the sum of A and B. (b) The off-diagonal component $\langle\sigma_{12}H\rangle_{av}=-\langle\sigma_{21}H\rangle_{av}$. Experimental average values, taken from Fig. 7, are shown for comparison.

$6.0\times10^{-8}H^2$ Ω cm if H is in kilogauss. Unfortunately the available data are only adequate to show that this estimate is not grossly in error. As for the magnitude of α, the following argument shows that it is not unreasonable. If zinc were a quasi-free-electron metal, with all electrons executing circular free-electron orbits in a magnetic field, the zero-field conductivity σ_0 could be written as $ne^2\tau/m^*$ and the cyclotron frequency ω_c as eH/m^*c, so that

$$[\omega_c\tau]_{\text{free}}=\sigma_0 H/nec\,,$$

with a value of 4.0 H for the specimen considered. This does not agree with the estimated mean value of $\omega_c\tau$ for the electrons and holes in zinc, which is $(\sigma_0/\alpha)^{1/2}H$, i.e. $22H$, but the discrepancy is of the expected order of magnitude. In the first place, the Brillouin zones lead to a reorganization of many of the free-electron orbits into smaller orbits, so that the average effective ω_c is much larger (probably by a factor approaching 3) than the free electron ω_c. Secondly the Fermi-surface area is not in reality as large as the free-electron surface, and the conductivity σ_0 is achieved by means of a value of τ correspondingly greater than the free-electron estimate. According to Fawcett[28] the real area is only 0.41 of the free-electron area, so that our estimate of $\omega_c\tau$ should be increased by a further factor 2.4. These two factors together could conceivably raise the original estimate from 4.0 H to 30 H, and there is a third effect which could raise it still further, the fact that the real orbits are not circular. This is probably not a very important effect, and is hard to estimate, but it is clear that there is no lack of scope to explain the observed effective $\omega_c\tau$.

The value of β is fixed by the unbalance of electrons and holes when breakdown is complete, and from the empirical value the total height of the breakdown zone is determined, using (3.8), as 3.6×10^{-2} atomic units (a.u.). This may be compared with the diameter of the waists of the monster, if these are assumed perfectly circular, of 3.9×10^{-2} a.u. The close agreement between these figures leaves little doubt of the correctness of our assumption that, as far as transport is concerned, it is the waists that determine the thickness of the slab in which breakdown is influential.

Finally, the breakdown field, 2.7 kG, needs discussion, since it is markedly different from the value of 6 kG estimated[14] from the amplitude of the de Haas–van Alphen effect. In fact this earlier estimate need not be taken seriously, since there is considerable latitude in the choice of H_0 if it is only the field-variation of amplitude that must be accounted for. According to the conventional theory, as used by Dhillon and Shoenberg,[29] if w is the amplitude of de Haas–van Alphen oscillations $wH^{3/2}\sinh X$ should give a linear graph when

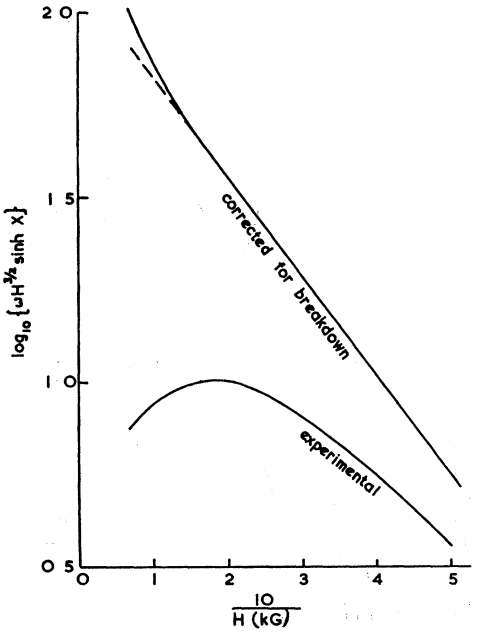

FIG. 9. The magnetic field dependence of the amplitude w of the de Haas–van Alphen effect in Zn (Ref. 29). In the absence of magnetic breakdown the curve should be a straight line. The experimental curve is corrected for breakdown, with a parameter $H_0=2.7$ kG.

plotted logarithmically against H^{-1}; this is well verified in bismuth, but not in zinc, as Fig. 9 shows. However, as shown in Refs. 14 and 30, the amplitude is reduced as a result of breakdown by a factor $Q^{3/2}$, so that the ordinates in Fig. 9 should be divided by $Q^{3/2}$ to allow for this.[31] When this is done, with $H_0=2.7$ kG, a very nearly linear plot is obtained. The departures at the highest fields need not cause much concern, since they might well be due to the needle not being ellipsoidal, as assumed in the theory of the amplitude, and departure from the ellipsoid will only appear in the amplitude of the last one or two oscillations. So we need not worry that $H_0=6$ kG gives an even better fit—with 2.7 kG the last oscillation has a correction factor of 13 and still falls off the straight line by only 25%, which is not unsatisfactory.

(*ii*) *Oscillations*

The breakdown zone in zinc is so narrow that unless the field strength is less than 1.4 kG the phase ϕ varies over the zone by less than 2π. Under these conditions the integral (3.6) must be computed numerically. This was done by dividing the complete interval $0<k_z<k_{zm}$ into 20 equally spaced segments in which the area of the needles varies between 4.26×10^{-5} a.u. and

[28] E. Fawcett, J. Phys. Chem. Solids 18, 320 (1961).
[29] J. S. Dhillon and D. Shoenberg, Phil. Trans. Roy. Soc. (London) A248, 1 (1955).
[30] L. M. Falicov and H. Stachowiak, Phys. Rev. 147, 505 (1966).
[31] Note that in this case the height of the breakdown zone is irrelevant; to reduce the amplitude of de Haas–van Alphen oscillations it is only necessary that the small orbit be coupled to other orbits—their character does not enter.

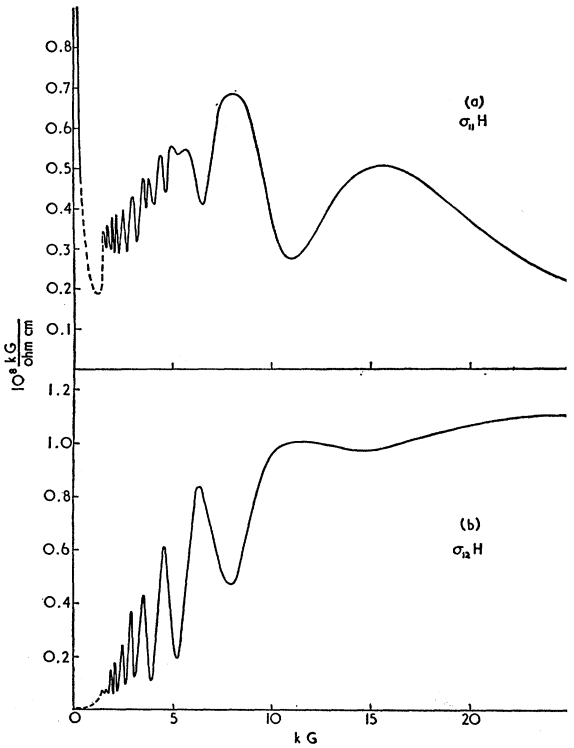

FIG. 10. The theoretical curves for σH in Zn corresponding to only one phase $\phi_0 = -3.84$. (a) $\sigma_{11}H = \sigma_{22}H$; (b) $\sigma_{12}H = -\sigma_{21}H$.

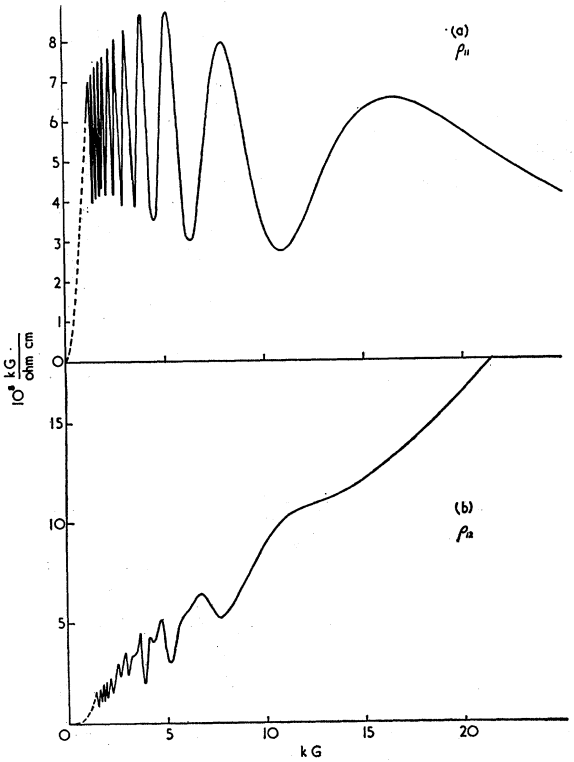

FIG. 11. The theoretical curves for the magnetoresistivity in Zn for one phase $\phi_0 = -3.84$, obtained by inverting the conductivity tensor of Fig. 10. (a) $\rho_{11} = \rho_{22}$; (b) $\rho_{12} = -\rho_{21}$.

3.55×10^{-5} a.u. The best fit to the over-all curves was obtained for a value of $\phi_0 = -3.84$. The resulting curves for σH and ρ are shown in Figs. 10 and 11. Comparison of these with Figs. 7 and 2 shows that although the over-all agreement is fair, the amplitude of the oscillation is larger in the theoretical curves than in the experimental ones. In addition the double-peak structure of the oscillations in σ_{21} cannot be reproduced by the theory as presented so far.

This structure was observed by Stark[1] and interpreted as evidence for a large effective g factor for the spins. Since then it has been studied in ultrasonic attenuation,[32] and a theoretical discussion by Bennett and Falicov[23] indicates that a value for g around 90 is quite plausible. Such a high value is necessary to split the Landau levels for the needles by anything comparable to their spacing, since the effective mass on these orbits is only 1/133 times the free electron mass. To incorporate spin-splitting into the theory all that is necessary is to assign half the amplitude of σH to each of two sets of oscillations characterized by different phase constants ϕ_0. Stark's suggestion that $g \sim 90$ corresponds to the two ϕ_0's differing by $\Delta\phi_0 \approx \frac{2}{3}\pi$, but this assignment need not be regarded as more than a rough estimate.

It is, of course, futile to expect spin-splitting to yield double-peaked behavior if the oscillations are strictly sinusoidal; all it can do is reduce the oscillatory amplitude by $\cos^2(\Delta\phi_0/2)$. However, if the field is not too large relative to H_0, the oscillations of $H\sigma$ are not sinusoidal, and the desired character can be produced. Examples of this are given in Fig. 12 from which it is clear that so long as Q is greater than about 0.4 a double-peaked oscillation can be constructed without too much loss in amplitude. At the lower fields, indeed, the theoretical spikiness is much stronger than what is observed, as also is the absolute amplitude of the oscillations. Even with the very small effective mass, however, the sharp peaks are sufficiently smoothed out by the temperature at fields of 2.3 kG for this not to present a serious problem. What is hard to understand is the persistence of the double-peaked character up to 15 kG, where $Q = 0.16$ if $H_0 = 2.7$ kG and both σ_{11} and σ_{21} oscillate almost strictly sinusoidally. It would be hard

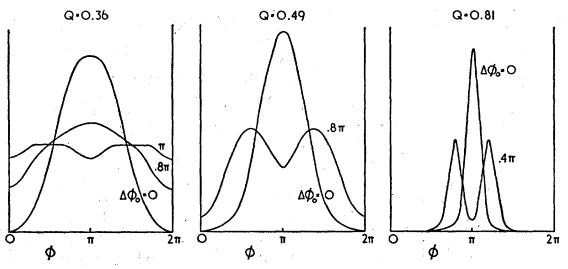

FIG. 12. The line shape of the oscillatory part of $\sigma_{21}H$ for various values of Q and the phase difference $\Delta\phi_0$.

[32] A. Myers and J. R. Bosnell, Phys. Letters 17, 9 (1965).

to increase H_0 above 3.5 kG without harming the agreement found for $\bar{\sigma}$, and it is equally unlikely that this good agreement could survive a variation of H_0 over a wide enough range in the breakdown zone to explain the oscillations. However, if these considerations are disregarded and the breakdown field H_0 is arbitrarily increased to 9.5 kG, Fig. 13 shows how the double-peak

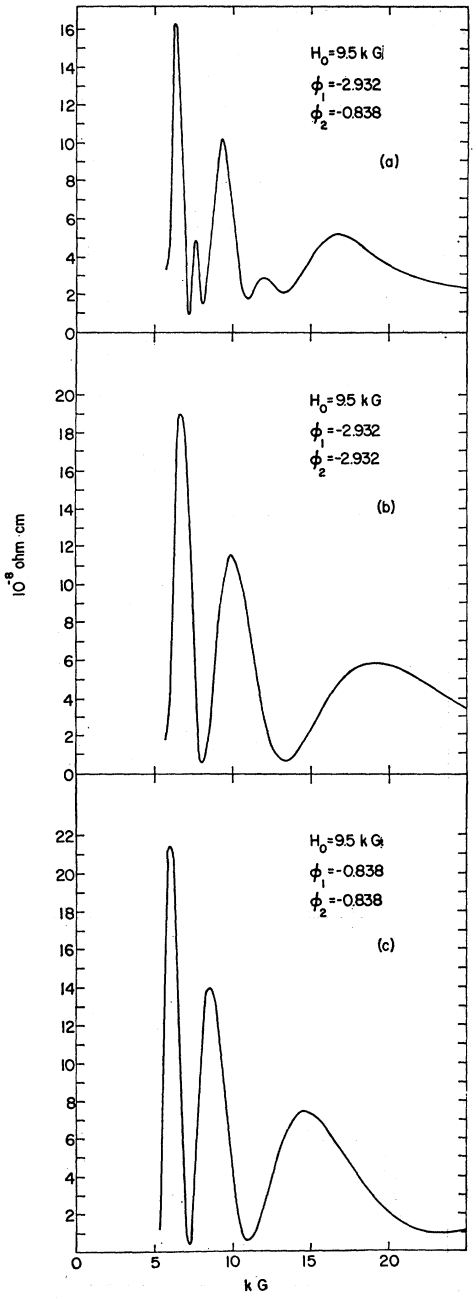

FIG. 13. The influence of the two phases ϕ_1 and ϕ_2 on the line shape of the magnetoresistance in Zn. The phases in (a) correspond to a $\Delta\phi=2\pi/3$ and a g factor of 89 or 178, while (b) and (c) correspond to $\Delta\phi=0$, $g=0$. In these three cases H_0 was taken to be 9.5 kG.

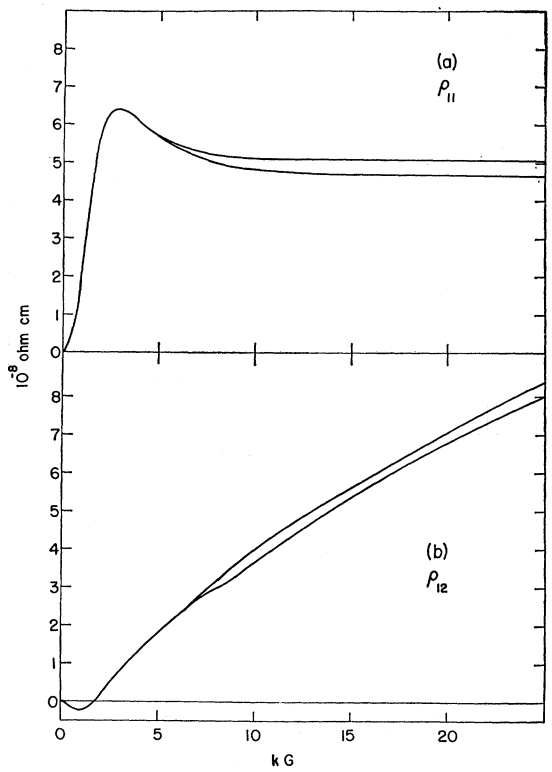

FIG. 14. Experimental curves for the transverse magnetoresistance and the Hall resistance in Mg for a magnetic field direction parallel to the hexad axis. The oscillations have been replaced by their envelopes. The curves were taken by R. W. Stark (Ref. 6) at 1.2°K in a sample not as pure as that of Fig. 1 (Ref. 6). (a) Transverse resistivity. (b) Hall resistivity.

structure appears as a consequence of the spin-splitting and a large g factor. We conclude therefore that although the theory in its present form, together with spin-splitting, go a long way towards accounting for the whole magnetoresistive behavior, there are points of detail which remain to be cleared up.

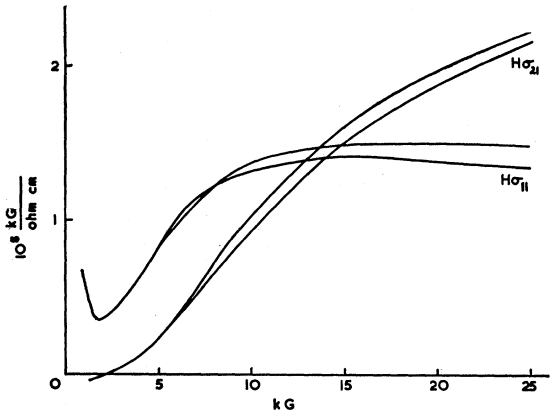

FIG. 15. The components of the product of the conductivity tensor and the magnetic field strength for Mg. The curves were obtained by direct inversion of the experimental curves of Fig. 14. The oscillations are replaced by their envelope.

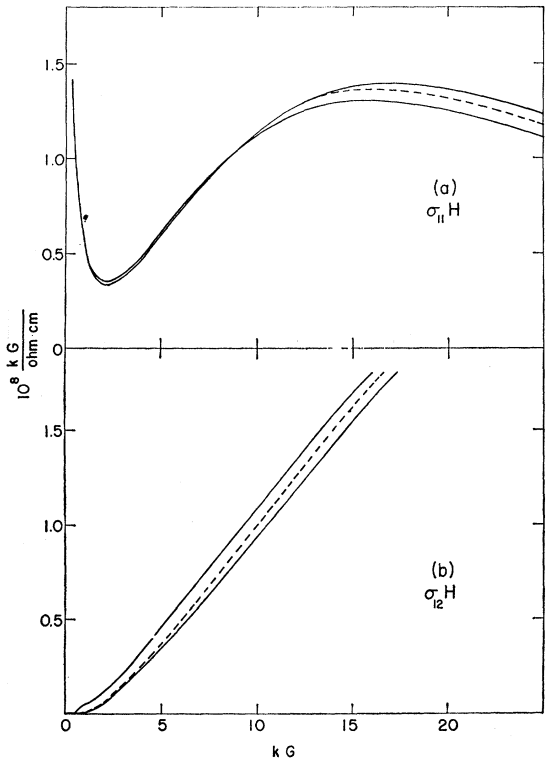

FIG. 16. Theoretical curves for the σH tensor in Mg for H_0 constant. (a) $\sigma_{11}H=\sigma_{22}H$; (b) $\sigma_{12}H=-\sigma_{21}H$. The full lines indicate the values for $\phi=0$ and $\phi=\pi$ and the dotted lines correspond to $\langle\sigma H\rangle_{av}$.

B. Magnesium

The needle (cigar) in Mg is considerably larger than in Zn, and the breakdown zone is also wider. A good fit between experiment and theory cannot be achieved by the use of a single parameter H_0, and even allowing H_0 to vary does not completely solve the problem.

In Fig. 14 and Fig. 15 the experimental results for ρ_{11} and ρ_{22}, and for σ_{11} and σ_{21} are, respectively, shown. Only the envelope of the oscillations is presented. In deriving the oscillatory part of σ from the measurements of ρ it is necessary to know whether ρ_{11} and ρ_{12} are in phase or in antiphase, and in this case the oscillations are of short enough period to make it hard to be certain purely from the experiments. Fortunately, however, the two possible choices lead to oscillations of σ on the complex plane which are quite differently oriented, one choice resulting in a pattern which accords closely with theoretical expectation (see e.g. the trajectories in Fig. 8 of Ref. 15), while the other would allow no interpretation within the assumed theoretical framework. We have not hesitated therefore to assume the desired phase relation in constructing Fig. 15.

The best fit to the experimental curve made by using a model with constant H_0, i.e. by means of (3.6), can be achieved by the following choice of parameters:

$$H_0=5.85\ \text{kG} \tag{4.3}$$

$$\alpha=0.52\times10^8\ \text{kG}^2/\Omega\ \text{cm},\qquad \beta=1.75\times10^8\ \text{kG}/\Omega\ \text{cm}, \tag{4.4}$$

$$\phi(0)=1.525\times10^4[H(\text{kG})]^{-1}. \tag{4.5}$$

The resulting curves for the conductivity and the resistivity are shown in Figs. 16 and 17, respectively. The values plotted there correspond to $\phi(0)=2n\pi$ and $\phi(0)=(2n+1)\pi$, which, for large H, coincide with the envelopes of the oscillations. Although the main features of the experimental data are reproduced, it is seen that the agreement can be considered only fair.

We shall attempt to obtain a better agreement by allowing H_0 to vary as a function of k_z. It is not convenient in this case to treat the average and the oscillatory parts of σ separately, since each provides information which restricts the choice of parameters.

From a comparison of Figs. 15 and 7 there is clearly a difference in the high-field behavior of Zn and Mg, in that $\langle\sigma_{11}H\rangle$ for Mg does not fall steadily beyond the peak, and $\langle\sigma_{21}H\rangle$ shows little tendency to saturate. Thus while the low-field behavior indicates breakdown well advanced at only a few kG, it is clearly still far from complete at 25 kG. There is reason to suppose a

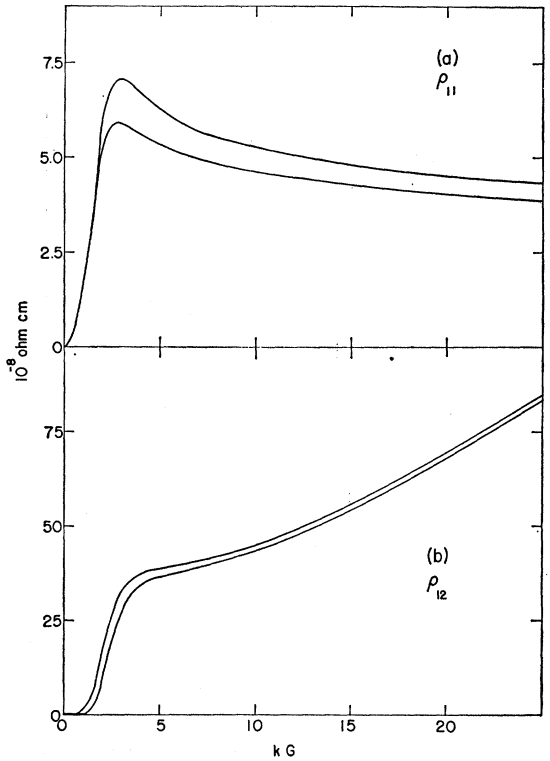

FIG. 17. Theoretical curves for the resistivity tensors in Mg obtained by inversion of the curves in Fig. 16. (a) $\rho_{11}=\rho_{22}$; (b) $\rho_{12}=-\rho_{21}$.

rather wide range of H_0 operative. Now the oscillations are dominated by a thin zone around the plane of extremal cross section of the cigars, presumably the central section, and we shall assume H_0 to be constant within this zone, using (3.11) and (3.12) to determine its value. We shall then attempt to find a plausible variation of H_0 with k_z that will account for the nonoscillatory part of σ.

The cyclotron mass of the cigar orbit is not so small as to allow temperature damping to be neglected, and the field variation of the oscillatory amplitude is not a very good starting point for the analysis. The "phase angle" of the oscillations, however, $\Delta\sigma_{11}/\Delta\sigma_{21}$ should not be altered by temperature effects, and we shall attempt to find H_{00}, the breakdown parameter at the center of the cigar, from the field variation of this ratio. In Fig. 18 the experimental curve is shown, together with a theoretical curve derived from Fig. 6, H_{00} being chosen as 5.3 kG. Agreement is only fair, but it must be remembered that, especially at the lower field strengths, it is hard to measure amplitudes exactly. Since the amplitudes are larger at the higher fields we have chosen H_{00} to fit theory and experiment here.

Having chosen H_{00} we now use (3.12) to compute the expected field variation of $\Delta\sigma$. Compounding the theoretical oscillation amplitude with the actually observed mean conductivity $\bar{\sigma}$, and inverting, we derive the expected oscillatory amplitude of ρ at 0°K. The field variation of $\Delta\rho_{11}$ (theoretical) is shown in Fig. 19 together with the observed amplitude. If the major part of the difference is to be attributed to the temperature (1.2°K), it is necessary to choose X to be about $15T/H$ °K/kG, corresponding to a cyclotron mass of the cigar orbit of 0.10 times the free-electron mass. This estimate agrees well with an estimate of 0.09 from temperature-variation of oscillatory amplitudes.[33] It is clear from Fig. 19 that over-all agreement is far from perfect, but without more experimental data it is unwise to speculate on the reason; one may rest reasonably satisfied that the interpretation is basically satisfactory.

The absolute magnitude of the oscillations deserves comment. It will be seen from Fig. 18 that the choice

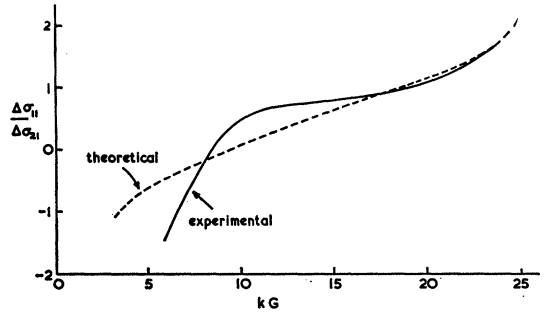

FIG. 18. Experimental and theoretical variations of the ratio $\Delta\sigma_{11}/\Delta\sigma_{21}$ with H.

[33] R. W. Stark (private communication).

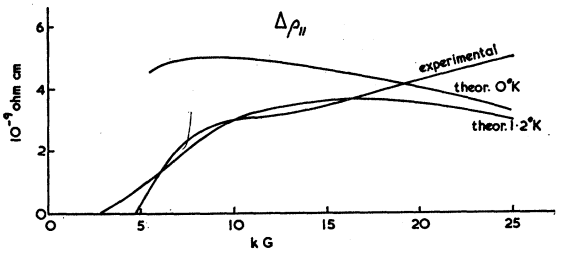

FIG. 19. Experimental and theoretical variations of $\Delta\rho_{11}$ with H.

of parameters has ensured rather close agreement between theory and experiment for $\Delta\sigma_{11}/\Delta\sigma_{21}$ at 17.5 kG, and from Fig. 19 that this is also a good field strength at which to fit $\Delta\rho_{11}$. To achieve this fit involves choosing the constant relating s to $H\Delta\sigma$, and hence from (3.12) the width W of the central zone. From (3.11) γ is then determined as 0.22, which may be compared with the free-electron value of 0.254 given in Table I. In view of the imperfect over-all fit this may be regarded as remarkable agreement; certainly the discrepancy does not deserve deep scrutiny.

We are now in a position to discuss the nonoscillatory variation of σ. If it is assumed that H_0 at the center of the cigars is 5.3 kG, it is clearly necessary, if Fig. 15 is to be explained, for H_0 to take larger values elsewhere in the breakdown zone. The next simplest assumption to taking H_0 as constant is to assume that the energy gap varies quadratically with k_z.

$$\Delta=\Delta_0(1+ak_z^2), \tag{4.6}$$

and therefore, from (1.2),

$$H_0=H_{00}(1+ak_z^2)^2. \tag{4.7}$$

We rule out negative values of a on the grounds that these would lead to a considerable width in the breakdown zone in which H_0 was so small that breakdown was complete even in weak fields. There is no evidence for such behavior in $\langle\sigma_{21}H\rangle_{\text{av}}$, which would under these

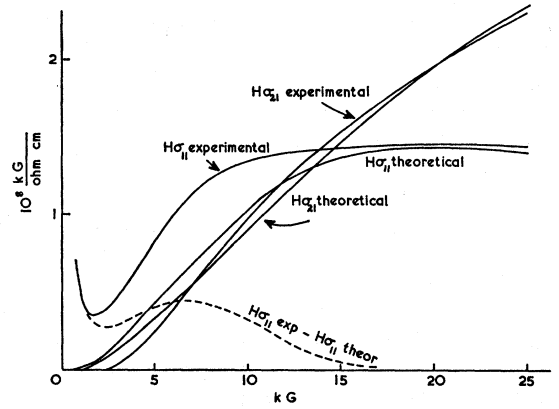

FIG. 20. Theoretical curves for the σH tensor in Mg for quadratic variation of $H_0(k_z)$. (a) $\sigma_{11}H=\sigma_{22}H$; (b) $\sigma_{21}H=-\sigma_{12}H$.

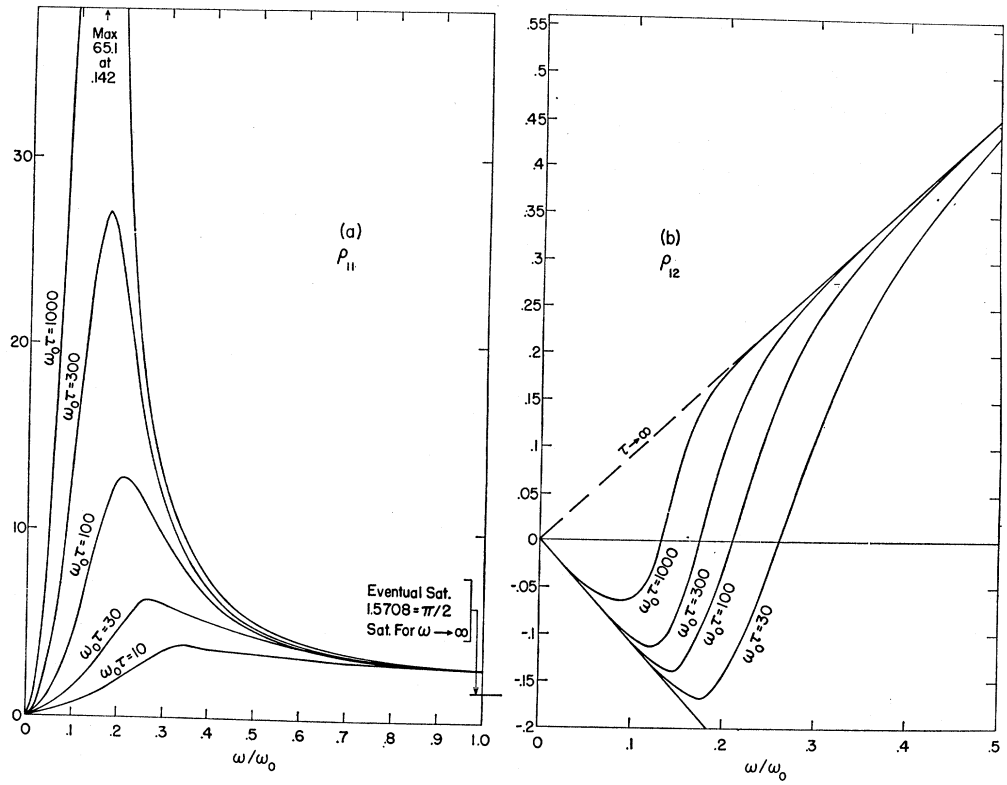

FIG. 21. The magnetoresistance and Hall resistance for a cylindrical slab of compensated hexagonal metal with (i) needles of finite size, of side length equal to the length of the hexagon side; (ii) finite relaxation times, (iii) no phase coherence. (a) The transverse resistivity in arbitrary units; (b) The Hall resistivity showing a hole-like region in a low field.

circumstances rise rather sharply at low fields. We assume therefore that H_0 varies monotonically, according to (4.4), from H_{00} at the center to H_{01} at the edges of the breakdown zone. The theoretical curves for $\langle\sigma_{11}H\rangle_{\rm av}$ and $\langle\sigma_{21}H\rangle_{\rm av}$ may readily be computed for different values of the ratio H_{01}/H_{00}. In order to choose an appropriate value we have elected to fit the ratio $\bar{\sigma}_{21}/\bar{\sigma}_{11}$ near the high-field end of the data, at 21.2 kG, i.e. 4 H_{00}. As H_{01}/H_{00} varies from 1 to 6 the theoretical value of $\bar{\sigma}_{21}/\bar{\sigma}_{11}$ varies from 1.96 to 1.28, and the experimentally determined ratio 1.43 corresponds to H_{01}/H_{00} being 2.5. It can be seen from Fig. 20 that the form of $\langle\sigma_{21}H\rangle_{\rm av}$ is rather well reproduced, but that the difference between theory and experiment in $\langle\sigma_{11}H\rangle_{\rm av}$ is not such as can be accounted for by a term of the form α/H contributed by closed orbits. We have not succeeded in finding an alternative set of parameters which will bring $\langle\sigma_{11}H\rangle_{\rm av}$ up rapidly at low fields without ruining the agreement for $\langle\sigma_{21}H\rangle_{\rm av}$; nor can we offer any explanation of the discrepancy. As in other comparisons, we must be content with a measure of agreement that indicates a fair understanding of the mechanisms at work, yet gives no excuse for complacency.

Before leaving the subject, there are two comments worth making. The first concerns the behavior of $\langle\sigma_{21}H\rangle_{\rm av}$ at low fields, where it reverses sign. At the higher fields, breakdown leads to an excess of electrons, but below about 1.5 kG, where breakdown is negligible, the character is hole-like. This is not hard to account for qualitatively. Consider for example a simple two-band metal containing n_e electrons and n_h holes, each behaving like free carriers but with different values of $\omega_c\tau$. The conductivity takes the form

$$\sigma=\frac{ec}{H}\left[\frac{n_e\chi_e}{1-i\chi_e}+\frac{n_h\chi_h}{1+i\chi_h}\right], \tag{4.8}$$

in which $\omega_c\tau$ is written as χ_e for electrons and χ_h for holes. Since the zero-field resistivity ρ_0 takes the form

$$\rho_0=\frac{H}{ec(n_e\chi_e+n_h\chi_h)}, \tag{4.9}$$

this can be written

$$\frac{\rho}{\rho_0}=[1+\chi_e\chi_h-i(\chi_e-\chi_h)]\times\frac{n_e\chi_e+n_h\chi_h}{n_e\chi_e+n_h\chi_h+i(n_e-n_h)\chi_e\chi_h}. \tag{4.10}$$

From this equation it can be seen that:

(a) If the metal is compensated, i.e. $n_e=n_h$, the Hall resistivity is given by

$$\mathrm{Im}\left[\frac{\rho}{\rho_0}\right]=-(\chi_e-\chi_h) \tag{4.11}$$

and its sign is determined by whichever carrier has the larger $\omega_c\tau$. Presumably in magnesium it is the holes which dominate, probably through the influence of the rather high cyclotron frequencies of the second-zone hole "monster."

(b) If we assume that the main effect of magnetic breakdown consists of a change of character of some orbits from hole-like to electron-like, i.e. n_e and n_h are functions of the magnetic field, the Hall effect will change sign when

$$n_e/n_h=(\chi_h^2/\chi_e^2)(1+\chi_e^2)/(1+\chi_h^2). \tag{4.12}$$

This equation is satisfied by a value of the magnetic field H_c which is a function of the cyclotron masses and relaxation times. It is easy to see that H_c increases as τ decreases, i.e. the crossover point in the Hall resistance is shifted upwards as the sample becomes "dirtier."

The model given above cannot of course be applied exactly to Mg, since at intermediate fields the effect of open orbits is of great importance, but the qualitative features are expected to remain. In order to prove this point we have calculated the magnetoresistance and Hall resistance of a cylindrical slab of hexagonal metal (Fig. 3) in which (1) the side of the triangular needle and the side of the hexagonal monster are equal, and equal to $\frac{1}{12}$ of the free-electron orbit; (2) the metal is compensated in the absence of magnetic breakdown, the compensating carriers being of the free electron type, electron-like character; (3) all phase coherence effects are completely neglected, only semiclassical effects being considered; (4) the relaxation time is finite and is the same for the various pieces of Fermi surface.

In this case we have used the matrix method of solving Boltzmann's equation[16] and the results are shown in Fig. 21. The hole-like Hall effect region is apparent and it is seen that it disappears as $\tau\rightarrow\infty$. It should be noted in passing that the finite size of the needles makes the over-all shape of the Hall-resistance curve resemble much more the experimental curve of Fig. 14(b).

The relaxation-time effect explains also why a hole-like region in the Hall effect was not detected experimentally by Stark[1] in Zn, while earlier experiments with dirtier samples[34] exhibited such a region for fields up to 5.5 kG. The second comment worth making is that the limiting value of $\langle\sigma_{21}H\rangle_{\mathrm{av}}$ at high fields determines the width of the breakdown zone. According to the model used, $\langle\sigma_{21}H\rangle_{\mathrm{av}}$ should saturate at 3.48×10^8 kG/Ω cm, corresponding to an excess of 2.18×10^{22} electrons/cm^3, and a breakdown zone of width 0.157 a.u. On the assumption that, as in Zn, it is the thinnest portion of the horizontal arms of the monster that demarcate the breakdown zone, we conclude that these arms must be noncircular; if they are elliptical they must have a height 2.6 times their width for their area to be consistent with the breakdown zone width. There is no obvious reason for doubting this result.

ACKNOWLEDGMENTS

We are very grateful to Professor R. W. Stark for communicating his results to us prior to publication and for many illuminating discussions at every stage of the present work.

Two of the authors (LMF and PRS) would like to acknowledge the direct financial support from the National Science Foundation, the Office of Naval Research, and the Advanced Research Project Agency and the partial support of related solid-state theory by the National Aeronautics and Space Administration.

[34] C. G. Grenier, J. M. Reynolds, and N. H. Zebouni, Phys. Rev. **129**, 1088 (1963).

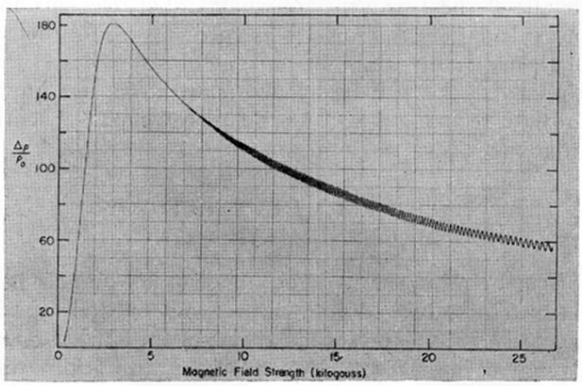

FIG. 1. A typical experimental curve for the transverse magnetoresistance in Mg for a magnetic field direction parallel to the hexad axis. The curve was taken by R. W. Stark (Refs. 5 and 6) in extremely high-purity Mg and does not include corrections for possible Hall effect contributions.